Available online at www.sciencedirect.com
ScienceDirect
Energy Reports 9 (2023) 577–583
www.elsevier.com/locate/egyr

2022 9th International Conference on Power and Energy Systems Engineering (CPESE 2022), Doshisha University, Kyoto, Japan, 9–11 September 2022

Impact of inertia response control strategy based doubly fed induction generator on frequency stability of power system

Jialin Zhang[a,*], Ping Wei[b], Xin Gao[a]

[a] *Xi'an Jiaotong University, iHarbor, Xi'an 710049, China*
[b] *Northwest Branch of State Grid Corporation of China, Xi'an 710049, China*

Received 18 October 2022; accepted 6 November 2022
Available online xxxx

Abstract

While the doubly fed induction generator (DFIG) is widely applied in the new power system, its decoupled control and fluctuation of output power have led to serious problems in frequency stability. Inertia response control (IRC) of DFIG has attracted significant attention, while its impact has not been clearly researched. In this study, a low-order model of DFIG focusing on frequency stability is proposed. Firstly, the simplified model of DFIG considering the IRC is introduced through Taylor series expansion. The frequency response model considering the energy storage system (ESS) is proposed. Taking the rate of change of frequency (RoCoF) and steady-state frequency deviation (SFD) as the constraint, an analytical solution for the maximum proportion of DFIGs is deduced to reflect the impact of IRC on the system frequency stability. Finally, the accuracy of the proposed method and the effectiveness of IRC is verified on the modified IEEE-9 system.

Peer-review under responsibility of the scientific committee of the 9th International Conference on Power and Energy Systems Engineering, CPESE, 2022.

Keywords: Doubly-fed induction generator; Transient frequency stability; Inertia response control; Frequency stability

1. Introduction

In the past few years, the requirement for sustainable social development and progress in long-distance power transmission systems have made the penetration of renewable energy grow steadily [1–3]. Among them, doubly fed induction generator (DFIG) has developed rapidly by its cleanness, high efficiency and flexible control. However, the uncertainty of its output power and low inertia results in the decreased reserve capacity and inertia of power system. The high proportion of DFIGs will bring in severe problems in the stability of system frequency. In the above context, the frequency stability of the high permeability DFIG power system is confronted with challenges. Therefore, it is of great significance to study the interaction between DFIG and the frequency stability of the system for guiding wind power source arrangement and maintaining the stability of the frequency [4–6].

* Corresponding author.
E-mail address: zhangjialin666@stu.xjtu.edu.cn (J. Zhang).

https://doi.org/10.1016/j.egyr.2022.11.084

Peer-review under responsibility of the scientific committee of the 9th International Conference on Power and Energy Systems Engineering, CPESE, 2022.

Frequency analysis on DFIG integrated power system has drawn great attention [7–9]. In [10], the quantitative estimation of the DFIG considering the frequency control is studied using Routh approximation and the least-squares algorithm, however, the high order DFIG model greatly increases the computational complexity. In [11], the frequency response model of DFIG is established, and the limit proportion of DFIG on the premise of system frequency stability is studied. In [12,13], the generalized model of DFIG is constructed, combined with the root locus method, the effect of the current loop controller parameters on the control performance of the system is studied.

This paper studies the correlation between wind power with inertia response control (IRC) and frequency stability. The maximum proportion of DFIG considering frequency constraints is deduced to evaluate the impact of IRC on DFIG integrated power system intuitively. Simulation results based on a modified IEEE-9 system demonstrates the effectiveness of the proposed method.

2. The transient frequency model of DFIG

2.1. Inertia response control

The inertia of power system depicts the amount of the rotating elements releasing or absorbing kinetic energy to compensate for the unbalanced power. The output power of the DFIG is determined by the maximum power point tracking control(MPPT), which depends on the wind speed and is decoupled from the system frequency [14]. Therefore, the DFIG does not equip with inertial response capability. However, by applying appropriate additional control to the DFIG, the rotating elements of the DFIG can still release or absorb kinetic energy to achieve a simulated inertial response when the system frequency changes, which is called IRC. At present, there are two methods to achieve the IRC of DFIG, one is to simulate the inertial response by modifying the maximum power tracking curve, and the other is to feedback the system frequency fluctuation through a proportional–derivative (PD) controller [15]. The output of the controller is superimposed on the reference value of active power given by MPPT. In the PD-type inertial response controller, the differential control is used to simulate the inertial response, and the proportional control essentially simulates a primary frequency modulation. Different from the primary frequency modulation of the traditional generator, DFIG has been running in the MPPT mode. The energy source of the primary frequency modulation is not the input mechanical power through the governor, but the kinetic energy of the wind turbine, so the primary frequency modulation of the DFIG is temporary.

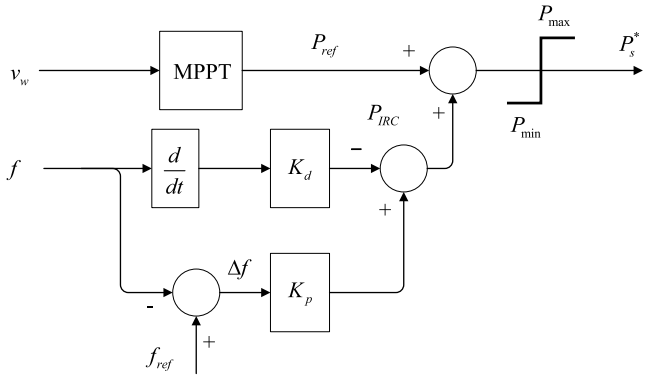

Fig. 1. Structure of IRC.

Fig. 1 is the structure of IRC, where f is the system frequency, V_w is the wind speed, which depends the active power reference value P_{ref} by MPPT. K_d is the derivative gain emulating inertia response of conventional generators, K_p is the proportional gain in the inertia response control to support the primary frequency modulation. The mathematical model is formulated below:

$$\begin{aligned} P_s^* &= P_{ref} + P_{IRC} \\ P_{IRC} &= k_p(f_{ref} - f) - k_d\frac{df}{dt} + P_{ref} \end{aligned} \tag{1}$$

2.2. Transient response model of DFIG

The transient response model of DFIG considering the IRC is studied in this section, the model without IRC can also be obtained when both k_p and k_d equal to 0 in following formulas.

The model of the DFIG is mainly composed of the wind turbine, transmission shaft, doubly-fed asynchronous generators, back-to-back converters and its control system. In [16], according to the eigenvalues analysis of the whole-system model, it is found that the latent roots about the rotor speed are close to imaginary axis while the other latent roots are far from the imaginary axis. This means when frequency fluctuates, only the variables about rotor speed play a dominant role. So, when only considering the frequency dynamic response characteristics of DFIG, the simplified model can be obtained:

$$\begin{aligned} &\frac{d\omega_r}{dt} = \frac{P_m - P_e}{2H_{wind}\omega_r} \\ &P_m = 0.5\rho\pi R^2 C_p \frac{V_w^3}{P_n} \\ &P_e = (1-d)\frac{k_{opt}\omega_r^3}{P_n} - (f - f_{ref})k_p - \frac{df}{dt}k_d \end{aligned} \tag{2}$$

where ω_r is the rotor speed, P_m is the mechanical power, P_e is the electric power, H_{wind} is the inertia time constant of the wind turbine, ρ is the air mass density, R is the rotor radius, C_p is the wind energy utilization gain which is determined by tip speed ratio $\lambda = \frac{\omega_r R}{V_w}$ and pitch angle β, P_n is the rated capacity of the DFIG, d is the deloading factor. The maximum active power of DFIG is multiplied by $(1-d)$ to reserve a certain spare capacity to participate in the primary frequency control. $k_{opt} = \frac{0.5\rho\pi R^5 C_{p\max}}{\lambda_0^3}$, where λ_0 is the blade tip speed ratio when operating at deloading factor d. k_{opt} stands for the MPPT control gain where the DFIG operating at maximum power point through adjusting ω_r. In this mode, the P_e and ω_r are approximately cubic, and β is maintained at 0 to capture the maximum wind energy.

For a nonlinear system of the form:

$$\begin{aligned} &\frac{dX}{dt} = g(X, Z) \\ &Y = f(X, Z) \end{aligned} \tag{3}$$

where g and f are nonlinear function, X denotes state variables, Z denotes input variables, Y denotes output variables. With Taylor series expansion, the first-order approximate linearized incremental equation of the above equation at the initial equilibrium point can be obtained:

$$\begin{aligned} &\frac{d\Delta X}{dt} = A\Delta X + B\Delta Z \\ &\Delta Y = C\Delta X + D\Delta Z \end{aligned} \tag{4}$$

where $A = \frac{\partial g}{\partial X}, B = \frac{\partial g}{\partial Z}, C = \frac{\partial f}{\partial X}, D = \frac{\partial f}{\partial Z}$. Through Laplace transform on Eq. (2), the following conversion relationship between ΔZ and ΔY can be deduced:

$$\Delta Y = [C(sI - A)^{-1}B + D]\Delta Z \tag{5}$$

In this paper, we select $X = [\omega_r]$ state variable, $Z = [f, \frac{df}{dt}]$ input variable and $Y = [P_e]$ output variable. The above matrix can be obtained: $A = [(k_m - k_e)/2H_{wind}\omega_r]$, $B = [k_p/2H_{wind}\omega_r, k_d/2H_{wind}\omega_r,]$, $C = [k_e]$, $D = [-k_p, -k_d]$, where $k_m = \frac{\partial P_m}{\partial \omega_r} = 0.5\rho\pi R^2 \frac{V_{w0}^3}{P_n}\frac{\partial C_p}{\partial \omega_r}$, $k_e = \frac{\partial P_e}{\partial \omega_r} = 3(1-d)\frac{k_{opt}\omega_{r0}^2}{P_n}$. The following relationship between the additional active power of DFIG and system frequency deviation is deduced during primary frequency control:

$$\frac{\Delta P_e}{\Delta f} = \frac{2H_{wind}\omega_r s - k_m}{2H_{wind}\omega_r s - (k_m - k_e)}(k_p + k_d s) \tag{6}$$

3. Calculation of maximum proportion of DFIG

According to [17], the system frequency response model can be obtained:

$$\begin{aligned} &2(1-K)H_{sys}\Delta f s = (1-K)\Delta P_G + K\Delta P_e + \Delta P_{ess} + \Delta P_d - D\Delta f \\ &\frac{\Delta P_G}{\Delta f} = \frac{K_{mg}(1+F_H T_R s)}{(1+T_R s)} K_g \end{aligned} \tag{7}$$

where K is the penetration rate of DFIG, H_{sys} denotes the inertia constant, D is the systematic damping, K_{mg} is the mechanical power gain factor, T_R is the turbine reheater time constant, F_H is the gain of high pressure cylinder, K_g is the frequency deviation coefficient of synchronous generator, ΔP_d is the unbalanced power caused by disturbance.

In [18,19], the multiplication of a first-order lag and a proportion gain is used to describe the characteristics of ESS when focusing on Frequency Regulation., the frequency response of ESS can be simplified as:

$$\frac{\Delta P_{ess}}{\Delta f} = \frac{K_{ess}}{T_{ess}s + 1} \tag{8}$$

where K_{ess} is the control gain, T_{ess} describe the delay effect of the ESS and power conversion system(PCS).

Combine the Eqs. (6) (8) (7), the frequency response model of the system can be deduced:

$$\begin{aligned} \Delta f = \Delta P_d / [&(1-K)\frac{K_{mg}(1+F_H T_R s)}{(1+T_R s)} K_g + K\frac{2H_{wind}\omega_r s - k_m}{2H_{wind}\omega_r s - (k_m - k_e)}(k_p + k_d s) + \frac{K_{ess}}{T_{ess}s+1} \\ &-D - 2(1-K)H_{sys}s] \end{aligned} \tag{9}$$

3.1. Considering the rate of change of frequency (RoCoF)

The RoCoF reflects the speed of frequency change when the system is disturbed. The RoCoF is an important indicator of dynamic frequency stability of the system, which relates to whether the system frequency reaches the dynamic safety limit. In the early stage of disturbance, since the speed governor of the synchronous generator has not yet acted, minimum frequency modulation resources can activate to frequency fluctuation, so RoCoF at this point should be the largest, which can be used as the system frequency constraint index. When there is an unbalanced power $\frac{\Delta P_d}{\Delta f} = \frac{P_D}{s}$, through Laplace's initial value theorem, the maximum RoCoF can be obtained as:

$$R_{\max} = \lim_{t\to+0}\frac{df}{dt} = \lim_{t\to+0}\frac{d\Delta f}{dt} = \lim_{s\to\infty} s(s\Delta f) = \frac{P_D}{2H_{sys} + K(k_d - 2H_{sys})} \tag{10}$$

It can be found that only the frequency regulation resources which provide instantaneous response such as synchronous generator and DFIG with inertia response control. On the contrary, the parameters of ESS have no effect on $R_{\max}$ for the delay effect of PCS.

Assume that the boundary of RoCoF is δ, the maximum Proportion of DFIG considering the RoCoF of the system can be obtained:

$$K_{\max,RoCoF} = \frac{2H_{sys} - \frac{P_D}{\delta}}{2H_{sys} - k_d} \tag{11}$$

3.2. Considering the steady-state frequency deviation (SFD)

The SFD has positive correlation with the primary frequency modulation capability of the system. Small SFD can reduce the secondary frequency control cost of the system, and the deviation of the frequency from the economic operating point is reduced. If the SFD of the system is too big, the risk of frequency collapse will increase when serious disturbance occurs. The SFD can be obtained through Laplace final value theorem:

$$R_\infty = \lim_{t\to\infty}\Delta f = \lim_{s\to 0}\Delta f = \lim_{s\to\infty} s\Delta f = \frac{P_D}{(K_{ess} + D + K_g K_{mg}(1-K)) + \frac{K k_m k_p}{(k_m - k_e)}} \tag{12}$$

Both control gain of ESS K_{ess} and proportional k_p have a positive influence on SFD, while the derivative gain is independent of SFD. The larger frequency deviation coefficient of the synchronous generator K_g can also improve

the SFD of the power system. When the limit of SFD is ε, the maximum Proportion of DFIG considering SFD can be deduced from Eq. (12):

$$K_{\max,SFD} = \frac{K_{ess} + D + K_g K_{mg} - \frac{P_D}{\varepsilon}}{K_g K_{mg} - \frac{k_m k_p}{k_m - k_e}} \tag{13}$$

Considering the above two constraints, take the smaller value as the maximum proportion of DFIG:

$$K_{\max} = \min(K_{\max,RoCoF}, K_{\max,SFD}) \tag{14}$$

4. Case study

4.1. Test system

The structure of test system is shown in Fig. 2, a modified IEEE RTS-9 system is built in Simulink to prove the accuracy of the frequency response model. Both the 50 MW ESS and 150 MW wind farm which are composed of several DFIGs are connected to the system at bus 3. The wind speed is kept at 9 m/s. Other detailed parameters of the system can be seen in [20]. The limit of RoCoF and SFD are chosen as 0.05 Hz/s and 0.2 Hz, respectively. The disturbance is set Bus 5.

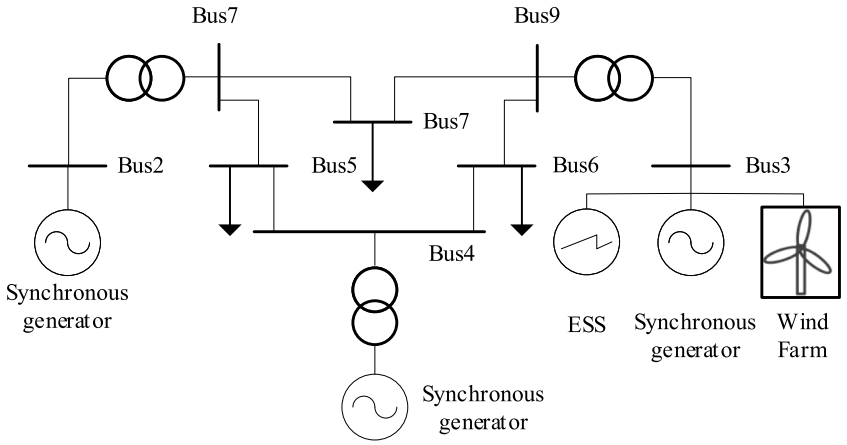

Fig. 2. The structure of test system.

4.2. The simulation results

In case 1, the $k_d = 1$ and $k_p = 10$. Change the load disturbance Pd as :8%, 10% and 12%. Through Eq. (14) the $K_{\max}$ can be calculated as 22.07%, 21.56% and 19.58%. Set the number of DFIGs to 67, 65 and 62 respectively. Record the system frequency response under disturbance. It can be seen in Fig. 3 that the SFD is around 0.2 Hz under Pd, and the RoCoF is below 0.05 Hz/s. The time domain simulation results prove the effectiveness of the proposed model. The larger scale of the load disturbance decreases the $K_{\max}$ considering the RoCoF and SFD limits (see Table 1).

Table 1. The calculation results.

Case 1	Pd = 8%	Pd = 10%	Pd = 12%
$K_{\max}$	22.07%	21.56%	19.58%
Case 2	$k_p = 0$	$k_p = 5$	$k_p = 10$
$K_{\max}$	17.93%	19.58%	21.56%

In case 2, the load disturbance is 10% of the system load. When $k_d = 1$ and $k_p = 0$, 5 and 10. Through Eq. (14) the $K_{\max}$ can be calculated as 17.93%, 19.58% and 21.56%. Set the number of DFIGs to 51, 57 and 64 respectively.

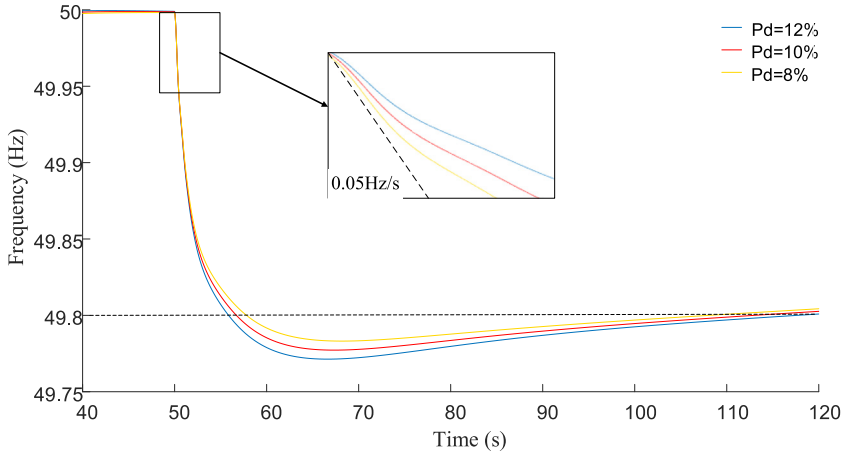

Fig. 3. The frequency response under different Pd.

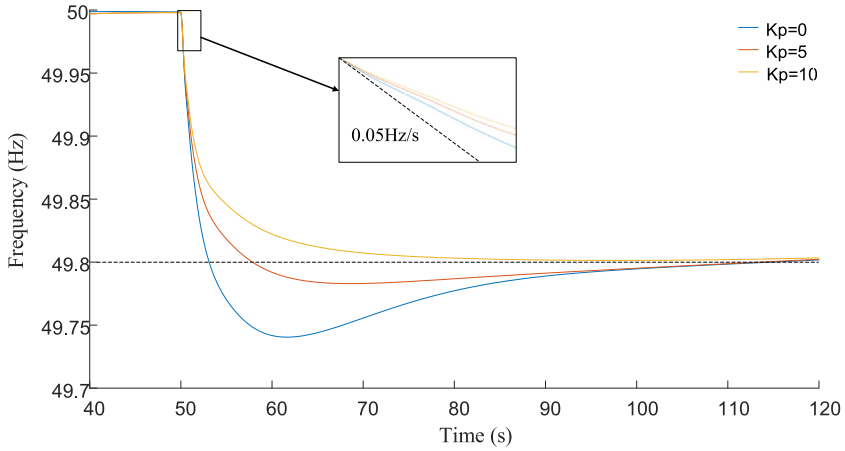

Fig. 4. The frequency response different Kp.

Record the system frequency response under disturbance. It can be seen in Fig. 4 that the SFD are also around the boundary. The RoCoF is within 0.05 Hz/s. As parameter k_p increases, the $K_{\max}$ increases gradually, that is, the frequency support capability of the DFIG increases.

5. Conclusion

In this paper, the impact of the IRC on frequency stability is studied through proposed low order DFIG model while considering the ESS in power system. It can be found out that The IRC can improve the RoCoF and the SFD while involve the DFIG in frequency regulation. The main factors affecting the frequency stability are load variation level, IRC parameters, system inertia constant and energy storage frequency modulation coefficient. Time domain simulation shows the validity of proposed model.

Declaration of competing interest

The authors declare the following financial interests/personal relationships which may be considered as potential competing interests: This work is supported by Science and Technology Foundation of State Grid Corporation Headquarters (Research on grid adaptation technology and support form of renewable energy stations suitable for new power system).

Data availability

The authors do not have permission to share data.

Acknowledgments

This work is supported by Science and Technology Foundation of State Grid Corporation Headquarter (Research on grid adaptation technology and support form of renewable energy stations suitable for new power system).

References

[1] Qin B, Liu W, Li H, Ding T, Ma K, Liu T. Impact of system inherent characteristics on initial-stage short-circuit current of MMC-based MTDC transmission systems. IEEE Trans Power Syst 2022;37.5:3913–22.
[2] Khan M, Zhang Y, Wang J, Wei J, Raza M, Ahmad A, Yuan Y. Determination of optimal parametric distribution and technical evaluation of wind resource characteristics for wind power potential at Jhimpir, Pakistan. IEEE Access 2021;9:70118–41.
[3] Ma J, Zhao D, Yao L, Qian M, Yamashita K, Zhu L. Analysis on application of a current-source based DFIG wind generator model. CSEE J Power Energy Syst 2018;4.3:352–61.
[4] Ochoa D, Martinez S. Fast-frequency response provided by DFIG-wind turbines and its impact on the grid. IEEE Trans Power Syst 2017;4002–11.
[5] Song Y, Blaabjerg F. Analysis of middle frequency resonance in DFIG system considering phase-locked loop. IEEE Trans Power Electron 2018;343–56.
[6] Huang J, Yang Z, Yu J, Liu J, Xu Y, Wang X. Optimization for DFIG fast frequency response with small-signal stability constraint. IEEE Trans Energy Convers 2021;2452–62.
[7] Qin B, Sun H, Ma J, Li W, Ding T, Wang Z, Zomaya A. Robust H∞ control of doubly fed wind generator via state-dependent riccati equation technique. IEEE Trans Power Syst 2019;34.3:2390–400.
[8] Zhang Y, Klabunde C, Wolter M. Frequency-coupled impedance modeling and resonance analysis of DFIG-based offshore wind farm with HVDC connection. IEEE Access 2020;147880-147894.
[9] Qin B, Ma J, Li W, Ding T, Sun H, Zomaya A. Decomposition-based stability analysis for isolated power systems with reduced conservativeness. IEEE Trans Autom Sci Eng 2020;17.3:1623–32.
[10] Chen P, Qi C, Chen X. Virtual inertia estimation method of DFIG-based wind farm with additional frequency control. J Mod Power Syst Clean Energy 2021;1076–87.
[11] Li S, Tang H, Deng C, Liu D, Shu Z, Zhong H. Calculation of wind power penetration limit involving frequency constraints and frequency regulation control of wind turbines. Autom Electr Power Syst 2019;33–43.
[12] Mei F, Pal B. Modal analysis of grid-connected doubly fed induction generators. IEEE Trans Energy Convers 2007;728–36.
[13] Qin B, Zhang R, Li H, Ding T, Liu W. Disturbance attenuation control for LVRT capability enhancement of doubly fed wind generators. IET Gener Trans Distrib 2021;15.18:2582–92.
[14] Zou Y, Elbuluk M, Sozer Y. Stability analysis of maximum power point tracking (MPPT) method in wind power systems. IEEE Trans Ind Appl 2013;1129–36.
[15] Zhu X, Wang Y, Xu L, X Zhang, Li H. Virtual inertia control of DFIG-based wind turbines for dynamic grid frequency support. In: IET conference on renewable power generation. 2011, p. 1–6.
[16] Lin J, Li G, Sun Y, Li X. Small-signal analysis and control system parameter optimization for DFIG wind turbines. Autom Electr Power Syst 2009;86–90.
[17] Anderson PM, Mirheydar M. A low-order system frequency response model. IEEE Trans Power Syst 1990;720–9.
[18] Mu Y, Wu J, Ekanayake J, Jenkins N, Jia H. Primary frequency response from electric vehicles in the great britain power system. IEEE Trans Smart Grid 2013;1142–50.
[19] Kim T, Qiao W. A hybrid battery model capable of capturing dynamic circuit characteristics and nonlinear capacity effects. IEEE Trans Energy Convers 2011;26(4):1172–80.
[20] Anderson PM. Power system control and stability. Iowa State University Press; 1977.